END
DATE
FILMED

DTIC

MICROCOPY RESOLUTION TEST CHART
NATIONAL BUREAU OF STANDARDS-1963-A

Laser-Plasma Interaction Experiments and Diagnostics at NRL

B. H. RIPIN, J. GRUN,* M. J. HERBST, S. T. KACENJAR,**
E. A. MCLEAN, S. P. OBENSCHAIN, J. A. STAMPER,
R. R. WHITLOCK,† AND F. C. YOUNG§

Laser·Plasma Branch
Plasma Physics Division

*Mission Research Corporation
Alexandria, VA

**NRL-NRC Postdoctoral Research Associate

†Condensed Matter Physics Branch
Condensed Matter and Radiation Sciences Division

§Plasma Technology Branch
Plasma Physics Division

May 11, 1983

NAVAL RESEARCH LABORATORY
Washington, D.C.

83 05 18 035

REPORT DOCUMENTATION PAGE		READ INSTRUCTIONS BEFORE COMPLETING FORM
1. REPORT NUMBER NRL Memorandum Report 5078	2. GOVT ACCESSION NO. AD·A128 254	3. RECIPIENT'S CATALOG NUMBER
4. TITLE (and Subtitle) LASER-PLASMA INTERACTION EXPERIMENTS AND DIAGNOSTICS AT NRL		5. TYPE OF REPORT & PERIOD COVERED Interim report on a continuing NRL problem.
		6. PERFORMING ORG. REPORT NUMBER
7. AUTHOR(s) B.H. Ripin, J. Grun,* M.J. Herbst, S.T. Kacenjar,** E.A. McLean, S.P. Obenschain, J.A. Stamper, R.R. Whitlock and F.C. Young		8. CONTRACT OR GRANT NUMBER(s)
9. PERFORMING ORGANIZATION NAME AND ADDRESS Naval Research Laboratory Washington, D.C. 20375		10. PROGRAM ELEMENT, PROJECT, TASK AREA & WORK UNIT NUMBERS DOE AI08-79DP 40092 (172); 47-0859-0-3; 47-1606-0-3
11. CONTROLLING OFFICE NAME AND ADDRESS U.S. Department of Energy Washington, D.C. 20545		12. REPORT DATE May 11, 1983
		13. NUMBER OF PAGES 30
14. MONITORING AGENCY NAME & ADDRESS(if different from Controlling Office)		15. SECURITY CLASS. (of this report) UNCLASSIFIED
		15a. DECLASSIFICATION/DOWNGRADING SCHEDULE

16. DISTRIBUTION STATEMENT (of this Report)

Approved for public release; distribution unlimited.

17. DISTRIBUTION STATEMENT (of the abstract entered in Block 20, if different from Report)

18. SUPPLEMENTARY NOTES

*Present address: Mission Research Corporation, Alexandria, VA
**NRL-NRC Postdoctoral Research Associate

(Continues)

19. KEY WORDS (Continue on reverse side if necessary and identify by block number)

Plasma
Diagnostics
Laser-produced plasma
Laser fusion
Plasma instabilities

20. ABSTRACT (Continue on reverse side if necessary and identify by block number)

Laser-plasma interaction experiments have now advanced to the point where very quantitative measurements are required to elucidate the physics issues important for laser fusion and other applications. Detailed time-resolved knowledge of the plasma density, temperature, velocity gradients, spatial structure, heat flow characteristics, radiation emission, etc. are needed over tremendous ranges of plasma density and temperature. Moreover, the time scales are very short, aggravating the difficulty of

(Continues)

DD FORM 1473 1 JAN 73 EDITION OF 1 NOV 65 IS OBSOLETE
S/N 0102-014-6601

18. SUPPLEMENTARY NOTES (Continued)

20. ABSTRACT (Continued)

the measurements further. Nonetheless, such substantial progress has been made in diagnostic development during the past few years that we are now able to do well diagnosed experiments.

In this paper the authors review recent diagnostic developments for laser-plasma interactions, outline their regimes of applicability, and show examples of their utility. In addition to diagnostics for the high densities and temperatures characteristic of laser fusion physics studies, diagnostics designed to study the two-stream interactions of laser created plasma flowing through an ambient low density plasma will be described.

CONTENTS

iii

LASER-PLASMA INTERACTION EXPERIMENTS AND DIAGNOSTICS AT NRL*

B.H. Ripin, J. Grun,[a] M.J. Herbst,
S.T. Kacenjar,[b] E.A. McLean, S.P. Obenschain
J.A. Stamper, R.R. Whitlock, and F.C. Young

Naval Research Laboratory
Washington, DC 20375
(a) Mission Research Corp., Alexandria, VA
(b) NRL/NRC Postdoctoral Research Associate

INTRODUCTION

Motivation for investigating the interaction of high-intensity laser light with targets include: basic physics studies, laser fusion, and the desire for unique high-energy-density plasma sources. Whatever the application, good diagnostics are needed to make advances. Diagnostic developments have expanded manyfold during the past few years, primarily because of the demanding requirements of laser fusion experiments. Simultaneous extremes in plasma density, temperature and space and time scales make this field very challenging.

In this article we will describe several diagnostics in use at NRL. Most of these have been developed to examine the properties of thin-planar targets which are accelerated to high speeds by laser induced ablation.[1-12] In these experiments we are trying to determine if targets, which emulate the outer shell of a laser fusion pellet, can be accelerated to high enough speeds ($> 2 \times 10^7$ cm/sec) with sufficient uniformity ($\delta v/v < 1\%$) and on a low enough isentrope ($T_p < $ few eV) to be useful for inertial fusion.[13] Moreover, high gain pellet burn requires that the total coupling efficiency from laser light into hydrodynamic energy be greater than about 5%. A suitable laser irradiance window for 1-μm laser light may exist in the low 10^{14} W/cm^2 range. We employ planar targets in our experiments since planar geometry affords

1

diagnostic advantages over pellets in observations of what would be the pellet inner wall and, for a given laser energy, can generate longer plasma scalelengths. Many results can be transferred to spherical geometry; however, neither spherical convergence nor ignition effects can be addressed. These issues and the diagnostic methods used to learn about them are discussed later.

Another NRL laser-plasma program, requiring a somewhat different set of instrumentation, uses high-velocity ($< 10^8$ cm/sec), cold ($\delta v/v < 0.3$) ablation plasma produced by laser irradiation of targets below 10^{14} W/cm^2.[14] An objective of this experiment is to examine the mechanisms responsible for the loss of momentum of this expanding plasma when it streams through low-density magnetized plasma; when atomic collisions are negligible, coupling between the two plasmas may occur through "collisionless" (plasma instability) mechanisms. The diagnostics in these studies overlap to some degree with those designed for laser fusion experiments. However, since the interaction between the two counter-streaming plasmas occurs at lower density and over larger volumes than the inertial fusion target accelerations, different diagnostics are needed.

We will describe the diagnostics in the context of the experiments in which they are used. The experiments and physics issues are briefly described along with the corresponding diagnostics and measurements. It is emphasized that this paper is not a review of all laser-plasma physics or diagnostics, or even of those for inertial fusion, but rather a small subset of those which we have found useful at NRL.

DESCRIPTION OF EXPERIMENTS

The NRL PHAROS II Nd-phosphate laser has a wavelength of 1.05 μm.[15] The beams output up to 500 J in 3-4 nsec pulses; experiments are performed by focusing the light onto thin planar targets placed in the quasi-near field of the f/6 aspheric focusing lens. For target experiments its two beams are usually combined using a polarizer into one beam. Focal spot diameters of between 100 μm and 2 mm are used depending upon the experiment at hand. The focal distribution and temporal history of the pulse are monotored on every shot. The laser intensity is uniform to $\pm$ 30% across the center of the focal spot unless intentionally structured. Sometimes only one beam of the laser is used to ablate the target with a 3-4 nsec multihundred joule laser pulse, while the other beam delivers about 25 J in a short pulse duration (< 300 psec). The short duration beam is used to generate x rays for x-ray backlighting or to irradiate the plasma created by the long pulse beam for interaction studies in large-scalelength plasmas.

2

The experimental arrangement for ablative acceleration of targets has been described extensively elsewhere.[1-12] Diagnostics monitor the scattered laser light, the plasma energy, velocity and momentum, x-ray emission spectra, underdense plasma density, and accelerated target temperature. X-ray backlighting allows imaging of the dense portions of the accelerating target and the double-foil method is able to measure velocity nonuniformities near the 1% level. Tracer dot techniques,[15-18] which are described in detail by Herbst et al.[18] in this volume, enables fluid flow visualization, improved spectroscopic observations and interpretations, and even velocity gradient determinations. Zeeman splitting of a helium-like CV spectral multiplet provides self-generated magnetic field information in the plasma near the target;[19] this method complements the Faraday rotation determinations.[20] In addition, a short-duration laser probe pulse, chopped out of the main oscillator pulse, is used for optical shadowgraphy, interferometry and scattering diagnostics.[21]

The same experimental arrangement described above is used in the momentum coupling experiments. However, instead of fully evacuating the chamber, a background gas surrounds the target; this gas is photoionized by the emission from the laser-target interaction and provides the stationary ambient plasma through which the laser-target debris streams. An external magnetic field can be applied across the interaction region by means of a magnet. In these experiments, additional diagnostics monitor the properties of the debris-ambient plasma interaction in the "coupling" region, which is typically within a few centimeters of the original target/focal region location. These diagnostics include: magnetic probes, ion time-of-flight detectors, spectrometers, framing cameras, and optical probe beams.

Next, the physics issues of ablative acceleration will be discussed; this will be followed by a brief description of the beam-plasma experiments.

LASER FUSION INTERACTION PHYSICS

The interaction physics of multi-nanosecond 1-μm laser pulses has favorable properties for accelerating material when laser intensities are below 10^{14} W/cm^2.[1,12] The laser light absorption, η_a, is high, typically 70-80%, and the energy is deposited in a thermal electron distribution of 300-1000 eV. Also, fast electron production and simulated Brillouin backscatter have been found to be negligible under these conditions. Ablation pressure scales with the 0.8 power of absorbed irradiance (P = 10 Mbar at I_a = 5 x 10^{13} W/cm^2); likewise the mass ablation rate, $\dot{m}$, and the ablation velocity, u, scale with the 0.6 and 0.2 powers of I_a respectively.[6,7] Hydrodynamic efficiencies, η_h, defined as the kinetic energy of the target divided by the absorbed energy, up to

20% were obtained in some cases. The pulse duration is long enough to establish approximately steady-state ablation. The laser focal spots are deliberately large (1 mm^2), to avoid the influence of edge effects,[2-7] and flat topped, to accelerate the target uniformly. The fluid flow of the ablating plasma,[16-18] mapped out by using the tracer dot method, is seen to be approximately one-dimensional and laminar in the ablating plasma acceleration region very near the target; at about a focal diameter from the target surface the fluid expansion becomes more spherical.

However, when 1-µm laser intensities exceed 10^{14} W/cm^2 the laser-plasma coupling begins to exhibit signs of detrimental high-irradiance effects. Increased backscatter, fast electron and ion production, self-generated magnetic fields, and so on, rear their ugly heads. To address these issues, especially under conditions approaching the long (mm's) density scalelengths of reactor pellets, we have undertaken two approaches:

1. Long density scalelengths in the target plasma are made by using a high energy (250 J) 3-nsec pulse with a big focal spot to create a large (250-600 µm) plasma. The interaction of a second, short-duration (~ 300 psec) and delayed pulse, which is focused to high intensity into the large expanding plasma, is observed. This approach allows high irradiance effects to occur in long scalelength plasmas with a minimum of laser energy. Initial results show increased direct backscatter over that seen with shorter scalelength plasmas, although the maximum backscatter through the focusing lens has not exceeded 25% for irradiances up to mid-10^{14} W/cm^2.

2. Multi-kilojoule, 3-nsec single-pulse experiments with large focal spots (1-mm) above 10^{14} W/cm^2 were performed jointly by NRL and LLNL on the (late) SHIVA laser.[23-24] The large laser spot size and energy creates large (600 µm) underdense plasmas. In this parameter regime the light absorption decreased to about 65% but the scattered light appeared uniformly distributed over 2π-sr. Three-halves harmonic light emission was below 1% and no signature of Raman scattering was seen. Moreover, the hot electron fraction increased to about 3% of the absorbed energy. It is speculated that a two-plasmon decay instability may be occurring here.

In both cases described above, changes in the interaction physics were seen above 10^{14} W/cm^2 in a large plasma which are undesirable for the laser fusion application. Although the

4

magnitude of these effects was small enough not to impact a reactor pellet's performance, the physics involved is not completely understood. More experiments in still larger plasmas are needed to predict behavior under reactor conditions.

Several recent advances in diagnostics have enabled us to characterize the underdense interaction plasma more completely.

Use of small tracer materials within the interaction region provides one of the most powerful techniques to characterize the underdense plasma. Small localized tracer materials embedded in the target surface are collisionally confined by, and flow out with, the blowoff plasma. When the spectral emission of the tracer material is imaged the flow properties of the plasma fluid are recorded. When the diameter of the tracer material flow-tube is correlated with a plasma density measurement, obtained, for example, with spectroscopy or interferometry, then flow velocity gradients are obtained; this method has resulted in the first inferences of the underdense plasma velocity profile (which is an important parameter in Brillouin backscatter calculations). Finally, plasma spectroscopy is significantly improved by using tracers as the spectroscopic source; source broadening, opacity effects, and the need to correct for integration along a plasma chord are greatly reduced. Complete density and temperature profiles from 2×10^{21}/cc to one-tenth critical density are obtained. The present status of the tracer method is discussed in detail in Herbst et al.[18]

Zeeman Splitting for Magnetic Field Measurements

Three methods have been used to measure magnetic fields in laser-produced plasmas: magnetic probes, Faraday rotation of laser probe light, and, recently, measurements of the Zeeman splitting of spectral lines emitted from ions in the laser plasma. Magnetic probes are useful for direct measurements of B in the lower density ($n_e < 10^{18}$/cc) regions of plasma. However, they suffer from being physically invasive and they are limited in spatial and temporal resolution. They perturb the plasma, and tend to be damaged in the high energy density environment of laser-produced plasmas. Faraday rotation of laser probe beams has provided measurements of megagauss level self-generated magnetic fields[20] at high density ($n_e = 10^{20}$/cc) and with good time resolution (~ 100 psec); however, the method requires a chord integration of Bn_e across the plasma and an independent measurement of the density profile is needed.

The third technique used to measure self-generated magnetic fields in the underdense plasma is from the Zeeman splitting of a helium-like multiplet (2271-2278 Å) of CV.[19] Using this technique, McLean et al. established that the self-generated

5

magnetic fields in our large focal spots are of order 100 kGauss
about 8 nsec after the laser pulse peak. As field strengths
increase above this level the Zeeman signature becomes easier to
discern and less dependent upon the specific assumptions of the
emission lines' self-absorption and Doppler shift. Figure 1 shows
the calculated line shapes of the multiplet for several magnetic
field strengths; the σ and π components are clearly different and
resolvable. Time-resolved observations were made of the line
emission in each of two polarizations and corrections for opacity
effects, Doppler shifts, instrumental and Stark broadening were
incorporated.

HIGH-SPEED UNIFORM-TARGET ACCELERATIONS

For most purposes an accelerated target must have a very
uniform velocity across its diameter; in fact, uniformities of the
order of 1% may be needed to achieve the high pellet compressions
required to give high gain performance. Many mechanisms can
degrade target acceleration uniformity. Kinematic mechanisms are
manifestations of a nonuniform pressure or mass: these include
nonuniformities in the incident beam which reach the ablation
surface (for which $\delta v \propto \delta P$)and accentuated versions in targets
which are thinning locally due to an intensity dependent mass
ablation rate. Care must be taken not to mistake the latter
effect for hydrodynamic instability since both cause velocity
variations which increase more rapidly than linearly in time.
Target areal density variations will also cause a kinematic
nonuniformity, or worse. Incident beam nonuniformities can be
accentuated by macroscopic refraction, self-focusing,
filamentation,[25] jetting[10,17] and magnetic fields,[20,26] in the
underdense plasma. Also, nonuniform heating of the target
interior can cause local blistering. All these effects can
potentially seed or enhance hydrodynamic instability. Conditions
that permit growth of hydrodynamic modes may occur at several
stages in the target acceleration-deceleration history. Rayleigh-
Taylor and Kelvin-Helmholtz modes may occur wherever a light fluid
is accelerating into a denser fluid; Benard convection cells may
develop in response to an inverted temperature gradient. In
addition to preventing a high density final state, hydrodynamic
instability can cause various layers in the target to mix and
degrade the performance.

Nonuniformities of accelerated targets can be observed
using: optical backlighting,[2] doppler reflectrometry,[8,27] double-
target collisions,[11] and x-ray backlighting.[28] The latter two are
emphasized here because they are sensitive to the high density (or
momentum carrying) portion of the target and they are capable of
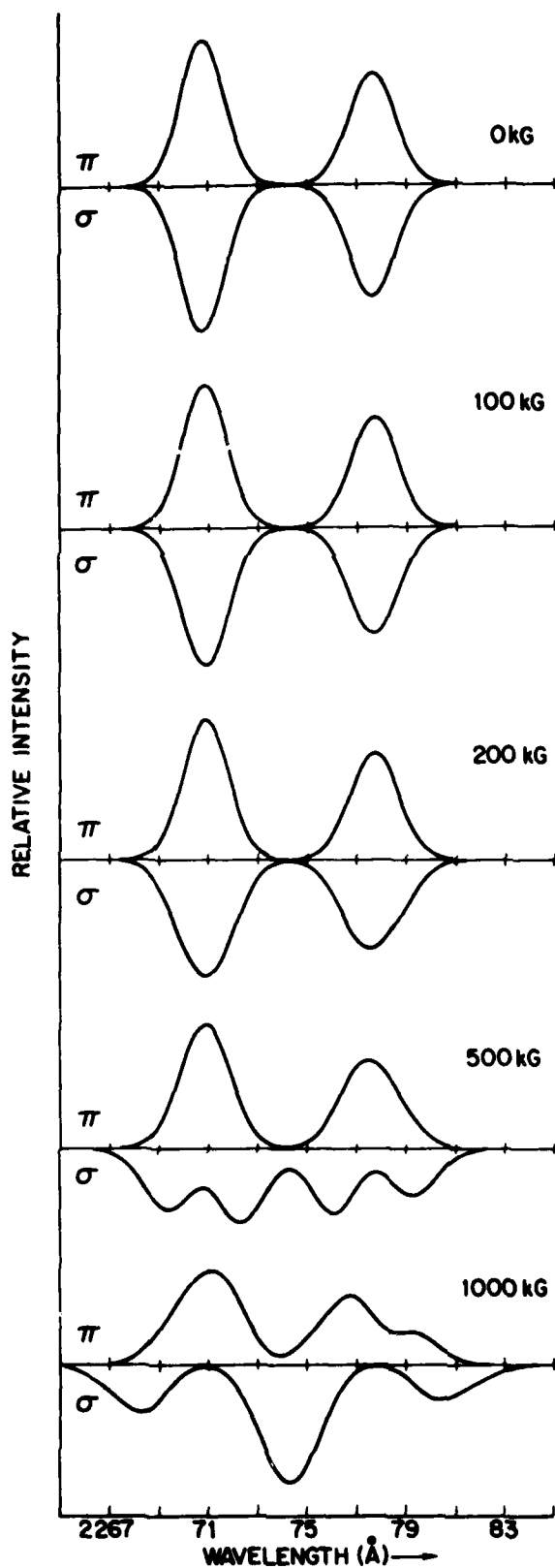discerning small nonuniformities (few %).

6

Figure 1. Zeeman splitting of helium-like CV multiplet as a function of magnetic field showing the σ and π components. Thermal and Stark broadening (1.6 Å) and instrumental broadening (0.75 Å) have been included.

7

Double-target Method

In the double-target method,[11,6,9] the collision of the accelerated target with a displaced diagnostic foil is observed across a diameter of the impacted foil rear surface with a streak camera, which time-resolves the visible light emission caused by impact. Nonuniformities in the target velocity profile are seen as time delays of the emission, observation of perturbations as small as 1% are feasible.[29]

The double foil-method has demonstrated the following features in targets accelerated with artificially introduced laser beam nonuniformities.

    o   Target velocity nonuniformities are substantially reduced over those of the applied laser beam intensity, and,

    o   Target velocity variations diminish with both increasing irradiance and decreasing perturbation scalelength.

For example, structure in the incident beam with a peak-to-valley distance of 140 μm ($\Lambda = 280$ μm) and 6:1 amplitude ratio result in only $\pm$ 10% target velocity variations at an average irradiance of 10^{13} W/cm^2.

The observed smoothing of the target velocity profile, relative to that of the incident beam, is believed to be due to the thermal heat diffusion between the absorption region, where the energy is deposited, and the ablation surface, where the bulk of the pressure is applied to the target. This "cloudy day" effect washes out hot spots when the distance d between absorption and ablation exceeds the perturbation scalelength Λ . Additional evidence that lateral thermal conduction can more effectively wash out beam nonuniformities with increasing irradiance and perturbation wave number is seen when the flow lines are mapped out in the ablating plasma by the tracer method.[17,29] Classical thermal transport in this region appears adequate to explain our present data for $I \lesssim 10^{14}$ W/cm^2. This inference is based on the agreement of hydrodynamic codes, assuming classical thermal conduction, with such experimental results as: target accelerations, ablation pressures and velocities,[6] and predictions of d which adequately explain the uniformity data.[29-32] The smoothing length d increases with laser irradiance and wavelength like $_I 0.7$ $_\lambda 2.7$ in a spherical model;[33] an analytic planar model[32] yields a similar scaling relation with $d \propto I^{4/3} \lambda^{13/4}$. These models adequately explain the observed enhanced smoothing with irradiance, and predict better smoothing with longer wavelength and increased irradiance.

To test whether uniformity actually continued to improve with irradiances above 3×10^{13} W/cm^2, experiments were done on the SHIVA facility where 3-4 kJ of 1.06 μm, 3 nsec laser light was focused onto 1 mm diameter areas (10^{14} W/cm^2) of planar carbon targets by overlapping 10 beams of the laser. Even though the light absorption fraction decreased to 65% and edge effects reduced the ablation pressure to 6 Mbar, the target velocity uniformity improved by more than a factor of two over the 3×10^{13} W/cm^2 case.[23] This improvement is expected from the cloudy day effect scaling. The corresponding double-foil uniformity measurement from the luminosity of the impact foil, shown in Fig. 2, demonstrates the excellent target uniformity obtained ($\lesssim \pm$ 3.5%) despite the 30% laser intensity variations thought to be placed on target. These results are summarized in Table I.
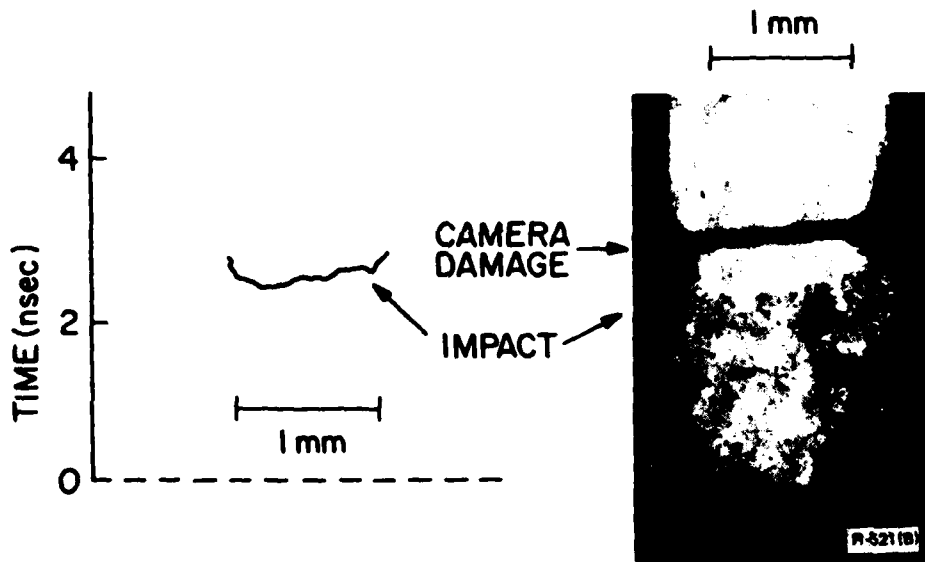
Figure 2. Double-target uniformity measurement at 10^{14} W/cm^2. The velocity uniformity inferred from these data is an 8% tilt, $\pm$ 3.5% nonuniformity across 800 μm and less than $\pm$ 2.5% across 200 μm scalelengths.

X-radiography

X-radiographs (x-ray backlighting) of the accelerated targets allow direct observation of the high density dynamics. These can be done in one of two generic ways. Either, two-dimensional projection can be obtained at discrete times by using a flash x-ray source with an imaging device, or, one-dimensional but

temporally continuous information may be obtained by imaging the object with an x-ray streak camera.

Flash x-radiographs of ablatively accelerated targets, such as the one shown in Fig. 3, show the high-density ($\rho > 0.03 \, \rho_{solid}$) regions of the intact target to be well-localized (40 µm) in space and show an acceleration uniformity in agreement with results of the double-foil method.[28] The target remains localized within the spatial resolution of the system (40 µm) even though the x-radiogram was taken at a time (+ 5 nsec) well after the end of the acceleration phase (the laser pulse is effectively over at + 2 nsec) where target decompression and disassembly can expand the target. Further measurements must be made to resolve the peak target densities and thicknesses beyond the limits already given. X-radiographs of accelerated targets in the double-target mode exhibit nonuniformities which corroborate the corresponding double-target inferences.
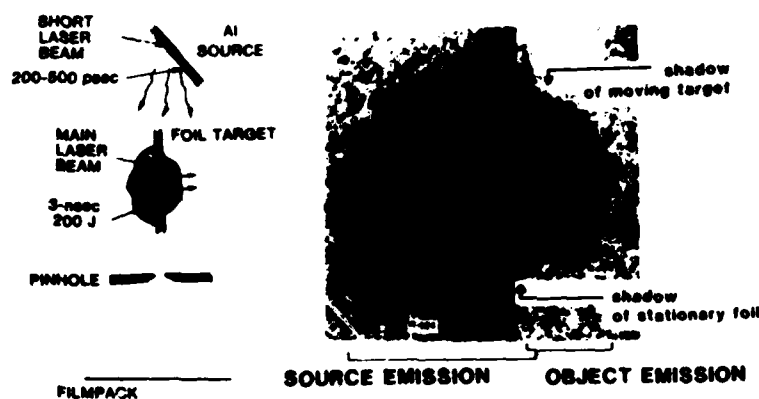
Figure 3. X-radiograph of an accelerated carbon target 5-nsec after the peak of the laser pulse.

A good example of the x-ray streak camera method is shown in Fig. 4; this image was obtained by R. Price of LLNL.[23,24] The collision of an ablatively accelerated target with an impact foil in a double-target assembly is backlit with 2.8-3.2 keV x rays from a palladium x-ray source. The final target velocity was above 10^7 cm/sec and the target clearly remained intact.

Structured Target for Rayleigh-Taylor Observation

Nonuniformities also result from target imperfections and hydrodynamic instability. These effects are examined experimentally in a manner analogous to those used in the beam uniformity studies, i.e., with purposely structured targets and

the use of the double-target method to infer the resulting velocity profile across the target diameter.[1] Several types of target perturbations are useful for these experiments, these include: ripples, areal-density variations, thickness variations, and mixtures of materials, to name a few, with adjustable initial wave lengths and amplitudes. Figure 5 shows some typical structured targets. In these experiments, the incident beam is made as smooth as possible to provide a uniform ablation pressure.
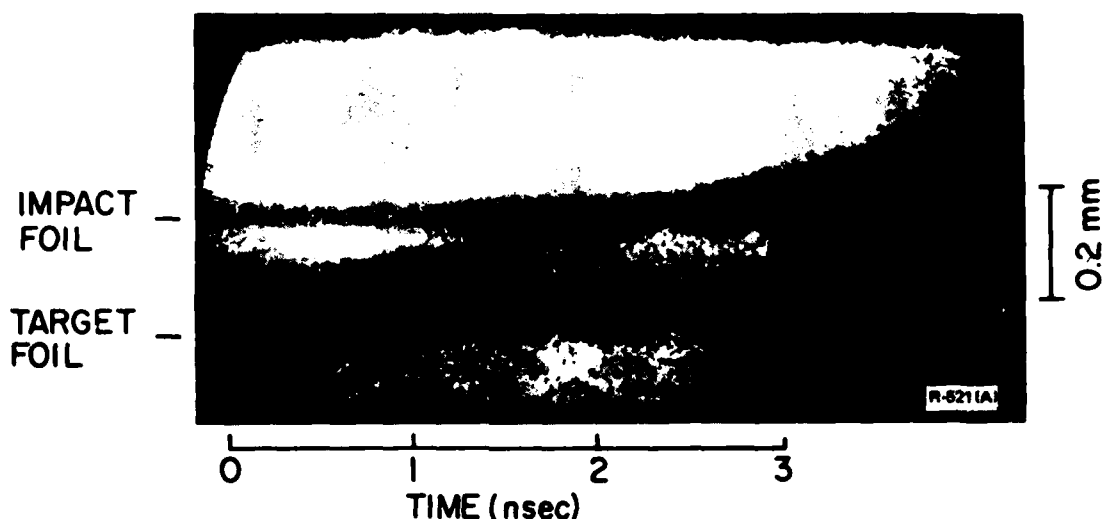
Figure 4. X-ray streak photograph of a double-target interaction.

The target structure resulting from an acceleration can be observed by a variety of techniques, although none are totally adequate to date. In the earliest experiment which utilized structured targets in a laser experiment, Ripin et al.[35,1] diagnosed the velocity nonuniformities resulting from rippled and stepped targets using the double-target method. Although the amplitude of the corresponding spatial nonuniformities grew by an order-of-magnitude as a result of the target accelerations, the observations can be explained by either hydrodynamic instability or kinematic effects.[1] To distinguish between these mechanisms diagnostics are needed which can either detect a characteristic signature of hydrodynamic instability, such as bubble-and-spike formation, or have the sensitivity and precision to follow the growth over several decades in amplitude. In the latter case one needs to perform an ultra-uniform acceleration over the spatial scale of the impressed structure; this may be achievable in future experiments by using laser irradiances over 10^{14} W/cm^2 or by using broad bandwidth laser beams with induced spatial incoherence.[36]
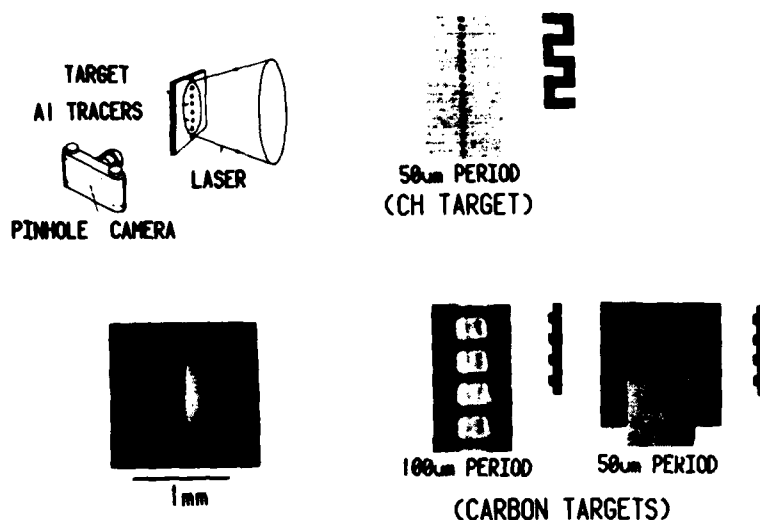
Figure 5. Sample structured targets for hydrodynamic stability experiments. The tracer dot method can be incorporated into these targets to make observations of turbulent ablation flow patterns.

One promising diagnostic approach to observe bubble-and-spike features is to use face-on x-radiography. This has been attempted using either a separate x-ray source,[37] or by incorporating the x-ray emitter into the target itself.[38] The latter method, devised by J. Grun of NRL, uses the x rays emitted from a thin layer of magnesium imbedded below the surface of a carbon target; a short duration x-ray burst, emitted as the Mg-layer is ablated, radiographs the target. Preliminary experiments show good signal-to-noise and a short x-ray burst duration (< 2 nsec).

Another approach, also due to Grun et al.,[38] mixes the tracer dot flow visualization method with structured targets. Figure 5 also shows examples of these targets. The tracer dot flow patterns should wash out if hydrodynamic turbulence occurs near the ablation surface due to, for example, bubble-spike or Kelvin-Helmholtz hammerhead formation.[39]

Target Preheat Measurements

Two methods have been used to measure the temperature (preheat) of the target material during acceleration. Time-resolved optical pyrometry monitors the optical emission from the rear of the target; this is related to temperature through

12

blackbody emission.[5] This technique has been used extensively for these measurements and the blackbody assumption has been verified. The other method, which has been used to corroborate the pyrometry, involves measuring the free-expansion velocity of the preheated material; it is termed the HA-method.[40] A knife edge replaces the impact target in a double-foil configuration (Half-Aft); it is designed to slice off the bottom half of the accelerated target as it passes the edge. The velocity of the lateral expansion of the freshly cut edge, u (cm/sec), is related to the internal temperature, T (eV), by

$$u = 3.8 \times 10^6 \, (ZT/A)^{1/2}, \qquad (1)$$

where Z/A is the charge-to-mass ratio of the target material. This method corroborated the optical pyrometry results.

For experiments done at NRL in the mid-10^{13} W/cm^2 irradiance regime and below, the major source of the observed preheat (< 10 eV) is from radiant heating due to x-ray emission below a few keV; this comes from the several-hundred electron volt plasma temperature in the interaction region.[5] There is little preheat dependence upon either target material or irradiance, but the temperature decreases with increased target thickness. This dependence is encouraging since a thicker target should be less susceptible to x-ray preheat.

The experiments done at 10^{14} W/cm^2 on SHIVA, however, exhibited temperatures up to 15 eV.[23] In this case the 3% hot electron (10 keV) population observed could account for the major portion of the preheat.

Although the preheat levels found in the target acceleration experiments are below 15 eV, it is desirable that they be further reduced for laser fusion. The thicker walls in reactor-sized targets should reduce the preheat to acceptable levels unless fast electrons increase too much in longer scalelength plasmas. Additionally, the use of very low-Z target materials (such as lithium, hydrogen, or beryllium) to reduce the radiant heat flux, the use of longer rise-time pulses to control shock-wave formation, and the use of target layers for x-ray and shock-wave shields are preheat-reducing measures that can be employed if needed.

ABLATIVE TARGET ACCELERATION SUMMARY

Thus far we have shown that dense targets can be ablatively accelerated to high speed. That is, targets have been accelerated to speeds of 160 km/sec at mid x 10^{13} W/cm^2 which are uniform to $\pm$ 7% and have temperatures less than 10 eV. Coupling efficiency of light into kinetic energy is high. Moreover, nonuniformities

present in the incident beam are increasingly damped out with higher irradiance and perturbation wave number. A summary of the target conditions found in our experiments at NRL is shown in Table I, they are within a factor of a few of those required for laser fusion. In the experiments with LLNL on the SHIVA laser it was verified that the acceleration uniformity improved further at 10^{14} W/cm^2, to better than $\pm$ 3.5%, and that the laser coupling physics remained benign.

Some additional factors that may be important but are not addressed here include: the effects of spherical geometry, wavelength scaling of the interaction physics and symmetrizing mechanisms and the effect of broad bandwidth laser illumination.

A spherical geometry effect that may be important is the possible reduction in hydrodynamic efficiency by up to a factor of 3 from the corresponding planar case.[41] The actual magnitude of this effect remains to be tested. There are also symmetry considerations that will be a function of spherical geometry. If the distance between laser light absorption and ablation decreases, due to the higher density gradient in three-dimensional versus planar expansion, then the unformity requirements increase for spherical geometry. Finally, effects of internal pressure of any material within the shell or the stability of the inner surface during the compression phases are not addressed in planar geometry, but indeed may present important symmetry issues for pellet implosions.

The scaling of the distance between absorption and ablation surfaces with laser wavelength has also not yet been fully explored experimentally. However, this "cloudy day" effect is generally thought to scale like $d \propto I^{0.7} \lambda^{2.7}$ from both analytic theory and numerical hydrodynamic code calculations. Thus, if additional symmetrization is required to reduce irradiation nonuniformities, a slightly longer laser wavelength may be desirable. Another approach is to increase laser irradiance, perhaps even with shorter wavelength radiation, and use broad-bandwidth and induced spatial incoherence to reduce laser beam nonuniformities and inhibit plasma instabilities.[36]

Another important set of questions to be answered, hopefully in the near future, relate to the scaling of the interaction physics and nonuniformity smoothing to larger systems, of several millimeter dimensions. In addition, the roles of target structural nonuniformity and hydrodynamic instability need further exploration.

14

Table I - Experimental status of ablative acceleration of
dense material to high velocity

Critical Element	NRL Experiments	NRL-LLNL Exp.[23]
Coupling Efficiency (total)	0.16	
absorption	0.8	$0.65 \pm 1.$
hydrodynamic	0.2	
Ablation Pressure	3 Mbar at $3 \times 10^{13} W/cm^2$	6 Mbar at $10^{14} W/cm^2$
target velocity	160 km/sec	100 km/sec
Target Isentrope	< 10 eV	~ 15 eV
Acceleration Uniformity		
$\delta v/v$	$\pm 7\%, \Lambda \sim 200 \ \mu m$	$\pm 3.5\%, \Lambda \sim 800 \ \mu m$
	$< \pm 2.5\%, \Lambda \sim 200 \ \mu m$	

INTERSTREAMING PLASMA INTERACTIONS

In these experiments, the ablated laser-target material is used as a high-velocity ($v_d \approx 7 \times 10^7$ cm/sec), but relatively cold ($\Delta T/T < 10\%$) plasma which streams through a low density ($n_e < 10^{16}$ cm^{-3}) stationary background plasma. Several beam-plasma instabilities can occur under these circumstances, especially in the presence of a magnetic field. The magnetized ion-ion instability[42] may occur under these conditions and effect a collisionless coupling between the two-plasma distribution functions and slow down the high-velocity laser-produced plasma. Diagnostics are needed to examine the conditions for the occurrence of these instabilities, the instability properties, the formation of magnetic shocks and bubbles in the externally applied magnetic field, etc. Thus, in addition to the aforementioned high-density laser-plasma diagnostics a new set is required for lower densities to study different physics issues.

A detailed discussion of the diagnostic set for the beam-plasma studies is outside the scope of this article and will appear elsewhere. Diagnostic methods that have been used to date include: temporally and spatially resolved atomic and molecular spectroscopy of the low density plasma, magnetic probes, optical interferometry and shadowgraphy, laser Thompson and resonant scattering, ion analysis, framing photography, and tracer material techniques.

REFERENCES

1. B.H. Ripin, S.E. Bodner, P.G. Burkhalter, H. Griem, J. Grun, H. Hellfeld, M.J. Herbst, R.H. Lehmberg, C.K. Manka, E.A. McLean, S.P. Obenschain, J.A. Stamper, R.R. Whitlock, and F.C. Young, Paper IAEA-CN-41/B-3, 9th Intl. Conf. on Plasma Physics and Controlled Nuclear Fusion Research, Baltimore, MD, 1-8 September 1982.

2. B.H. Ripin, R. Decoste, S.P. Obenschain, S.E. Bodner, E.A. McLean, F.C. Young, R.R. Whitlock, C.M. Armstrong, J. Grun, J.A. Stamper, S.H. Gold, D.J. Nagel, R.H. Lehmberg, and J.M. McMahon, NRL Memo Report #3890 (1978); Phys. Fluids 23, 1012 (1980) and 24, 990 (1981).

3. R. Decoste, S.E. Bodner, B.H. Ripin, E.A. McLean, S.P. Obenschain, and C.M. Armstrong, Phys. Rev. Lett. 42, 1673 (1979).

4. B.H. Ripin, R.R. Whitlock, F.C. Young, S.P. Obenschain, E.A. McLean, and R. Decoste, Phys. Rev. Lett. 43, 350 (1979).

5. E.A. McLean, S.H. Gold, J.A. Stamper, R.R. Whitlock, H.R. Griem, S.P. Obenschain, B.H. Ripin, S.E. Bodner, M.J. Herbst, S.J. Gitomer, and M.K. Matzen, Phys. Rev. Lett. 45, 1246 (1980).

6. J. Grun, R. Decoste, B.H. Ripin, and J. Gardner, Appl. Phys. Lett. 39, 545 (1981).

7. J. Grun, S.P. Obenschain, B.H. Ripin, R.R. Whitlock, E.A. McLean, J. Gardner, M.J. Herbst, and J.A. Stamper, NRL Memo Report #4747 (1982); accepted for publication in Phys. Fluids.

8. S.P. Obenschain, R.H. Lehmberg, and B.H. Ripin, Appl. Phys. Lett. 37, 903 (1980).

9. S.P. Obenschain, J. Grun, B.H. Ripin, and E.A. McLean, Phys. Rev. Lett. 46, 1402 (1981).

10. M.J. Herbst, R.R. Whitlock, and F.C. Young, Phys. Rev. Lett. 47, 91 (1981); Phys. Rev. Lett. 47, 1568 (1981).

11. B.H. Ripin, S.E. Bodner, S.H. Gold, R.H. Lehmberg, E.A. McLean, J.M. McMahon, S.P. Obenschain, J.A. Stamper, R.R. Whitlock, F.C. Young, H.R. Griem, J. Grun, and M.J. Herbst, NRL Memo #4212 (1980).

12. B.H. Ripin, S.E. Bodner, J. Grun, M.J. Herbst, E.A. McLean, J.M. McMahon, S.P. Obenschain, J.A. Stamper, R.R. Whitlock, and F.C. Young, Ultraviolet and UVU Systems, Proc. SPIE 279, 46 (1981).

13. S.E. Bodner, J. Fusion Energy 1, 221 (1981).

14. B.H. Ripin et al., Bull. Am. Phys. Soc. 27, 1041 (1982).
15. J.M. McMahon et al., IEEE J. Quant. Elec. QE17, 1629 (1981).
16. M.J. Herbst and J. Grun, Phys. Fluids 224, 1917 (1981); M.J. Herbst, P.G. Burkhalter, J. Grun, R.R. Whitlock, and M. Fink, Rev. Sci. Insts. 53, 1418 (1982).
17. M.J. Herbst, R.R. Whitlock, J.A. Stamper, R.H. Lehmberg, F.C. Young, J. Grun, and B.H. Ripin, Proc. of Symmetry Aspects of Inertial Fusion Implosions, NRL Report (1981).
18. M.J. Herbst, P. G. Burkhalter, D. Duston, M. Emery, J. Gardner, J. Grun, S.P. Obenschain, B.H. Ripin, R.R. Whitlock, J.P. Apruzese, and J. Davis, pg. , this volume.
19. E.A. McLean, J.A. Stamper, H.R. Griem, C.K. Manka, D.W. Droemer, and B.H. Ripin (to be published).
20. J.A. Stamper and B.H. Ripin, Phys. Rev. Lett. 34, 138 (1975).
21. An extensive review of optical probing techniques for laser-plasma interaction experiments is included in: J.A. Stamper, E.A. McLean, S.P. Obenschain, and B.H. Ripin, to be published.
22. M.J. Herbst, P.G. Burkhalter, J. Grun, S.P. Obenschain, J.A. Stamper, F.C. Young, E.A. McLean, B.H. Ripin, and R.R. Whitlock, NRL Memo #4893 (1982).
23. S.P. Obenschain, R.R. Whitlock, E.A. McLean, B.H. Ripin, R.H. Price, D. Phillion, E.M. Campbell, M.D. Rosen, and J.M. Auerbach, Phys. Rev. Lett. 50, 44 (1983).
24. E.M. Campbell et al., Proc. of IEEE Intl. Conf. on Plasma Science, IEEE Cat. #82CH1770-7, 55 (1982) to be published.
25. M.J. Herbst, J.A. Stamper, R.R. Whitlock, R.H. Lehmberg, and B.H. Ripin, Phys. Rev. Lett. 46, 328 (1981).
26. J.A. Stamper, E.A. McLean, and B.H. Ripin, Phys. Rev. Lett. 40, 1177 (1978).
27. S.P. Obenschain, E.A. McLean, and S.H. Gold, Rev. Sci. Instr. 51, 1661 (1980).
28. R.R. Whitlock, S.P. Obenschain, J.M. McMahon, B.H. Ripin, and J.A. Sprague, Proc. of Symmetry Aspects of Inertial Fusion Implosions, NRL Report (1981); R.R. Whitlock, S.P. Obenschain, and J. Grun, Appl. Phys. Lett. 41, 429 (1982); R.R. Whitlock, S.P. Obenschain, J. Grun, J.A. Stamper, and B.V. Sweeney, Proc. of SPIE/15th Intl. Congress on High Speed Photography and Photonics, San Diego, CA (1982).
29. S.P. Obenschain, J.A. Stamper, E.A. McLean, M.J. Herbst, S.E. Bodner, R.H. Lehmberg, J.M. McMahon, J. Grun, R. R. Whitlock, and B.H. Ripin, Proc. of Symmetry Aspects of Inertial Fusion Implosions, NRL Reort (1981).
30. M.H. Emery, J.H. Gardner, J.P. Boris, and J.H. Orens, NRL Memo #4500 (1981).
31. M.H. Emery and J.H. Gardner, Phys. Rev. Lett. 48, 677 (1982).
32. W.M. Manheimer, D.G. Colombant, and J.H. Gardner; Phys. Fluids 25, 1644 (1982).
33. J.H. Gardner and S.E. Bodner, Phys. Rev. Lett. 47, 1137 (1981).

34. R.H. Price, E.M. Campbell, M.D. Rosen, J.M. Auerbach, D.W. Phillion, R.R. Whitlock, S.P. Obenschain, E.A. McLean, and B.H. Ripin, Proc. of SPIE/15th Intl. Congress on High Speed Photography and Photonics, San Diego, CA (1982); also Lawrence Livermore Laboratory Report UCRL-87158 (1982).
35. B.H. Ripin et al., Bull. Am. Phys. Soc. $\underline{25}$, 946 (1980).
36. R.H. Lehmberg and S.P. Obenschain (to be published).
37. A. Cole, J. Kilkenny, P. Rumsby, M. Key, C. Hooker, and S. Knight in Rutherford Laboratory Report RL-82-039 (1982).
38. J. Grun, M.H. Emery, M.J. Herbst, E.A. McLean, S.P. Obenschain, B.H. Ripin, J.A. Stamper, and R.R. Whitlock, NRL Memo Report #4896 (1983).
39. M. Emery, et al., IAEA-CN-41/W-9 (1981); M.H. Emery, J.H. Gardner, and J.P. Boris, Phys. Rev. Lett. $\underline{48}$, 677 (1982); see also NRL Memo Report #4882 (1982).
40. B.H. Ripin, E.A. McLean, and J.A. Stamper, Phys. Fluids $\underline{25}$, 2128 (1982).
41. S.E. Bodner, pg.   , this volume.
42. K. Papadopoulos, R. Davidson, J.M. Dawson, I. Haber, D.A. Hammer, N.A. Krall, and R. Shanny, Phys. Fluids $\underline{14}$, 849 (1971).

University of California
Lawrence Livermore National Lab
Post Office Box 808
Livermore, CA 94550
   H.G. Ahlstrom, L-481
   J.L Emmett, L-448
   J.F. Holzrichter, L-481
   M.J. Monsler, L-479
   J.H. Nuckolls, L-477
   L.W. Coleman, L-473
   J.T. Hunt, L-481
   A.B. Langdon, L-477

U.S. Department of Energy
Office of Inertial Fusion
Washington, DC 20545
   L.E. Killian
   G. Gibbs
   T.F. Godlove
   S.L. Kahalas
   J.E. Lewis
   R.L. Schriever
   T.H. Walsh
   S.J. Barish

U.S. Dept. of Energy (194 cys)
Technical Information Center
P.O. Box 62
Oak Ridge, TN 37830

Defense Tech. Information Ctr. (2 cys)
Cameron Station
5010 Duke Street
Alexandria, VA 22314

R. McCrory
University of Rochester
250 East River Road
Rochester, NY 14623

Robert T. Duff
U.S. Department of Energy
Office of Classification
Washington, DC 20545

Rex B. Purcell (2 cys)
U.S. Department of Energy
Nevada Operations Office
Post Office Box 14100
Las Vegas, NV 89114

Z.N. Zafiris/R. Bredderman
U.S. Department of Energy
San Francsico Operations Office
1333 Broadway
Oakland, CA 94512

Los Alamos National Laboratory
Post Office Box 1663
Los Alamos, NM 87545
   S.D. Rockwood, ICF Prog. Mgr.
   DAD/IF, M/S527 (6 cys)

G. Yonas (4 cys)
Sandia National Laboratories
Post Office Box 5880
Albuquerque, NM 87185

S. Bodner
Naval Research Laboratory
Code 4730
Washington, DC 20375

T. Coffey
Naval Research Laboratory
Code 1001
Washington, DC 20375

Alexander Glass
KMS Fusion, Inc.
3941 Research Park Drive
P.O. Box 1567
Ann Arbor, MI 48106

NRL Code 4700 (26 cys)

NRL Code 4730 (100 cys)

NRL Code 2628 (20 cys)

DEPARTMENT OF DEFENSE

ASSISTANT SECRETARY OF DEFENSE
COMM, CMD, CONT 7 INTELL
WASHINGTON, D.C. 20301

DIRECTOR
COMMAND CONTROL TECHNICAL CENTER
PENTAGON RM BE 685
WASHINGTON, D.C. 20301
  01CY ATTN C-650
  01CY ATTN C-312 R. MASON

DIRECTOR
DEFENSE ADVANCED RSCH PROJ AGENCY
ARCHITECT BUILDING
1400 WILSON BLVD.
ARLINGTON, VA. 22209
  01CY ATTN NUCLEAR MONITORING RESEARCH
  01CY ATTN STRATEGIC TECH OFFICE

DEFENSE COMMUNICATION ENGINEER CENTER
1860 WIEHLE AVENUE
RESTON, VA. 22090
  01CY ATTN CODE R410
  01CY ATTN CODE R812

DEFENSE TECHNICAL INFORMATION CENTER
CAMERON STATION
ALEXANDRIA, VA. 22314
  02CY

DIRECTOR
DEFENSE NUCLEAR AGENCY
WASHINGTON, D.C. 20305
  01CY ATTN STVL
  04CY ATTN TITL
  01CY ATTN DDST
  03CY ATTN RAAE

COMMANDER
FIELD COMMAND
DEFENSE NUCLEAR AGENCY
KIRTLAND, AFB, NM 87115
  01CY ATTN FCPR

DIRECTOR
INTERSERVICE NUCLEAR WEAPONS SCHOOL
KIRTLAND AFB, NM 87115
  01CY ATTN DOCUMENT CONTROL

JOINT CHIEFS OF STAFF
WASHINGTON, D.C. 20301
  01CY ATTN J-3 WWMCCS EVALUATION OFFICE

DIRECTOR
JOINT STRAT TGT PLANNING STAFF
OFFUTT AFB
OMAHA, NB 68113
  01CY ATTN JLTW-2
  01CY ATTN JPST G. GOETZ

CHIEF
LIVERMORE DIVISION FLD COMMAND DNA
DEPARTMENT OF DEFENSE
LAWRENCE LIVERMORE LABORATORY
P.O. BOX 808
LIVERMORE, CA 94550
  01CY ATTN FCPRL

COMMANDANT
NATO SCHOOL (SHAPE)
APO NEW YORK 09172
  01CY ATTN U.S. DOCUMENTS OFFICER

UNDER SECY OF DEF FOR RSCH & ENGRG
DEPARTMENT OF DEFENSE
WASHINGTON, D.C. 20301
  01CY ATTN STRATEGIC & SPACE SYSTEMS (OS)

WWMCCS SYSTEM ENGINEERING ORG
WASHINGTON, D.C. 20305
  01CY ATTN R. CRAWFORD

COMMANDER/DIRECTOR
ATMOSPHERIC SCIENCES LABORATORY
U.S. ARMY ELECTRONICS COMMAND
WHITE SANDS MISSILE RANGE, NM 88002
  01CY ATTN DELAS-EO F. NILES

DIRECTOR
BMD ADVANCED TECH CTR
HUNTSVILLE OFFICE
P.O. BOX 1500
HUNTSVILLE, AL 35807
  01CY ATTN ATC-T MELVIN T. CAPPS
  01CY ATTN ATC-O W. DAVIES
  01CY ATTN ATC-R DON RUSS

PROGRAM MANAGER
BMD PROGRAM OFFICE
5001 EISENHOWER AVENUE
ALEXANDRIA, VA 22333
  01CY ATTN DACS-BMT J. SHEA

CHIEF C-E- SERVICES DIVISION
U.S. ARMY COMMUNICATIONS CMD
PENTAGON RM 1B269
WASHINGTON, D.C. 20310
  01CY ATTN C- E-SERVICES DIVISION

COMMANDER
FRADCOM TECHNICAL SUPPORT ACTIVITY
DEPARTMENT OF THE ARMY
FORT MONMOUTH, N.J. 07703
  01CY ATTN DRSEL-NL-RD H. BENNET
  01CY ATTN DRSEL-PL-ENV H. BOMKE
  01CY ATTN J.E. QUIGLEY

COMMANDER
HARRY DIAMOND LABORATORIES
DEPARTMENT OF THE ARMY
2800 POWDER MILL ROAD
ADELPHI, MD 20783
    (CNWDI-INNER ENVELOPE: ATTN: DELHD-RBH)
  01CY ATTN DELHD-TI M. WEINER
  01CY ATTN DELHD-RB R. WILLIAMS
  01CY ATTN DELHD-NP F. WIMENITZ
  01CY ATTN DELHD-NP C. MOAZED

COMMANDER
U.S. ARMY COMM-ELEC ENGRG INSTAL AGY
FT. HUACHUCA, AZ 85613
  01CY ATTN CCC-EMEO GEORGE LANE

COMMANDER
U.S. ARMY FOREIGN SCIENCE & TECH CTR
220 7TH STREET, NE
CHARLOTTESVILLE, VA 22901
  01CY ATTN DRXST-SD
  01CY ATTN R. JONES

COMMANDER
U.S. ARMY MATERIAL DEV & READINESS CMD
5001 EISENHOWER AVENUE
ALEXANDRIA, VA 22333
  01CY ATTN DRCLDC J.A. BENDER

COMMANDER
U.S. ARMY NUCLEAR AND CHEMICAL AGENCY
7500 BACKLICK ROAD
BLDG 2073
SPRINGFIELD, VA 22150
  01CY ATTN LIBRARY

DIRECTOR
U.S. ARMY BALLISTIC RESEARCH LABORATORY
ABERDEEN PROVING GROUND, MD 21005
  01CY ATTN TECH LIBRARY EDWARD BAICY

COMMANDER
U.S. ARMY SATCOM AGENCY
FT. MONMOUTH, NJ 07703
  01CY ATTN DOCUMENT CONTROL

COMMANDER
U.S. ARMY MISSILE INTELLIGENCE AGENCY
REDSTONE ARSENAL, AL 35809
  01CY ATTN JIM GAMBLE

DIRECTOR
U.S. ARMY TRADOC SYSTEMS ANALYSIS ACTIVITY
WHITE SANDS MISSILE RANGE, NM 88002
  01CY ATTN ATAA-SA
  01CY ATTN TCC/F. PAYAN JR.
  01CY ATTN ATTA-TAC LTC J. HESSE

COMMANDER
NAVAL ELECTRONIC SYSTEMS COMMAND
WASHINGTON, D.C. 20360
  01CY ATTN NAVALEX 034 T. HUGHES
  01CY ATTN PME 117
  01CY ATTN PME 117-T
  01CY ATTN CODE 5011

COMMANDING OFFICER
NAVAL INTELLIGENCE SUPPORT CTR
4301 SUITLAND ROAD, BLDG. 5
WASHINGTON, D.C. 20390
  01CY ATTN MR. DUBBIN STIC 12
  01CY ATTN NISC-50
  01CY ATTN CODE 5404 J. GALET

COMMANDER
NAVAL OCCEAN SYSTEMS CENTER
SAN DIEGO, CA 92152
  03CY ATTN CODE 532 W. MOLER
  01CY ATTN CODE 0230 C. BAGGETT
  01CY ATTN CODE 81 R. EASTMAN

DIRECTOR
NAVAL RESEARCH LABORATORY
WASHINGTON, D.C. 20375
  01CY ATTN CODE 4700 S. L. Ossakow
        26 CYS IF UNCLASS. 1 CY IF CLASS)
  01CY ATTN CODE 4701
  01CY ATTN CODE 4780 BRANCH HEAD
  01CY ATTN CODE 7500
  01CY ATTN CODE 7550
  01CY ATTN CODE 7580
  01CY ATTN CODE 7551
  01CY ATTN CODE 7555
  01CY ATTN CODE 4730 E. MCLEAN
  01CY ATTN CODE 4187

COMMANDER
NAVAL SEA SYSTEMS COMMAND
WASHINGTON, D.C. 20362
  01CY ATTN CAPT R. PITKIN

COMMANDER
NAVAL SPACE SURVEILLANCE SYSTEM
DAHLGREN, VA 22448
  01CY ATTN CAPT J.H. BURTON

OFFICER-IN-CHARGE
NAVAL SURFACE WEAPONS CENTER
WHITE OAK, SILVER SPRING, MD 20910
  01CY ATTN CODE F31

DIRECTOR
STRATEGIC SYSTEMS PROJECT OFFICE
DEPARTMENT OF THE NAVY
WASHINGTON, D.C. 20376
  01CY ATTN NSP-2141
  01CY ATTN NSSP-2722 FRED WIMBERLY

COMMANDER
NAVAL SURFACE WEAPONS CENTER
DAHLGREN LABORATORY
DAHLGREN, VA 22448
  01CY ATTN CODE DF-14 R. BUTLER

OFFICER OF NAVAL RESEARCH
ARLINGTON, VA 22217
  01CY ATTN CODE 465
  01CY ATTN CODE 461
  01CY ATTN CODE 402
  01CY ATTN CODE 420
  01CY ATTN CODE 421

COMMANDER
AEROSPACE DEFENSE COMMAND/DC
DEPARTMENT OF THE AIR FORCE
ENT AFB, CO 80912
  01CY ATTN DC MR. LONG

COMMANDER
AEROSPACE DEFENSE COMMAND/XPD
DEPARTMENT OF THE AIR FORCE
ENT AFB, CO 80912
  01CY ATTN XPDQQ
  01CY ATTN XP

AIR FORCE GEOPHYSICS LABORATORY
HANSCOM AFB, MA 01731
  01CY ATTN OPR HAROLD GARDNER
  01CY ATTN LKB KENNETH S.W. CHAMPION
  01CY ATTN OPR ALVA T. STAIR
  01CY ATTN PHP JULES AARONS
  01CY ATTN PHD JURGEN BUCHAU
  01CY ATTN PHD JOHN P. MULLEN

AF WEAPONS LABORATORY
KIRTLAND AFT, NM 87117
  01CY ATTN SUL
  01CY ATTN CA ARTHUR H. GUENTHER
  01CY ATTN NTYCE 1LT. G. KRAJEI

AFTAC
PATRICK AFB, FL 32925
  01CY ATTN TF/MAJ WILEY
  01CY ATTN TN

AIR FORCE AVIONICS LABORATORY
WRIGHT-PATTERSON AFB, OH 45433
  01CY ATTN AAD WADE HUNT
  01CY ATTN AAD ALLEN JOHNSON

DEPUTY CHIEF OF STAFF
RESEARCH, DEVELOPMENT, & ACQ
DEPARTMENT OF THE AIR FORCE
WASHINGTON, D.C. 20330
  01CY ATTN AFRDQ

HEADQUATERS
ELECTRONIC SYSTEMS DIVISION/XR
DEPARTMENT OF THE AIR FORCE
HANSCOM AFB, MA 01731
  01CY ATTN XR J. DEAS

HEADQUATERS
ELECTRONIC SYSTEMS DIVISION/YSEA
DEPARTMENT OF THE AIR FORCE
HANSCOM AFB, MA 01732
  01CY ATTN YSEA

HEADQUATERS
ELECTRONIC SYSTEMS DIVISION/DC
DEPARTMENT OF THE AIR FORCE
HANSCOM AFB, MA 01731
  01CY ATTN DCKC MAJ J.C. CLARK

COMMANDER
FOREIGN TECHNOLOGY DIVISION, AFSC
WRIGHT-PATTERSON AFB, OH 45433
  01CY ATTN NICD LIBRARY
  01CY ATTN ETDP B. BALLARD

COMMANDER
ROME AIR DEVELOPMENT CENTER, AFSC
GRIFFISS AFB, NY 13441
  01CY ATTN DOC LIBRARY/TSLD
  01CY ATTN OCSE V. COYNE

SAMSO/SZ
POST OFFICE BOX 92960
WORLDWAY POSTAL CENTER
LOS ANGELES, CA 90009
  (SPACE DEFENSE SYSTEMS)
  01CY ATTN SZJ

STRATEGIC AIR COMMAND/XPFS
OFFUTT AFB, NB 68113
  01CY ATTN XPFS MAJ B. STEPHAN
  01CY ATTN ADWATE MAJ BRUCE BAUER
  01CY ATTN NRT
  01CY ATTN DOK CHIEF SCIENTIST

SAMSO/SK
P.O. BOX 92960
WORLDWAY POSTAL CENTER
LOS ANGELES, CA 90009
  01CY ATTN SKA (SPACE COMM SYSTEMS)
       M. CLAVIN

SAMSO/MN
NORTON AFB, CA 92409
(MINUTEMAN)
  01CY ATTN MNNL LTC KENNEDY

COMMANDER
ROME AIR DEVELOPMENT CENTER, AFSC
HANSCOM AFB, MA 01731
  01CY ATTN EEP A. LORENTZEN

DEPARTMENT OF ENERGY
LIBRARY ROOM G-042
WASHINGTON, D.C. 20545
  01CY ATTN DOC CON FOR A. LABOWITZ

DEPARTMENT OF ENERGY
ALBUQUERQUE OPERATIONS OFFICE
P.O. BOX 5400
ALBUQUERQUE, NM 87115
  01CY ATTN DOC CON FOR D. SHERWOOD

EG&G, INC.
LOS ALAMOS DIVISION
P.O. BOX 809
LOS ALAMOS, NM 85544
  01CY ATTN DOC CON FOR J. BREEDLOVE

UNIVERSITY OF CALIFORNIA
LAWRENCE LIVERMORE LABORATORY
P.O. BOX 808
LIVERMORE, CA 94550
  01CY ATTN DOC CON FOR TECH INFO DEPT
  01CY ATTN DOC CON FOR L-389 R. OTT
  01CY ATTN DOC CON FOR L-31 R. HAGER
  01CY ATTN DOC CON FOR L-46 F. SEWARD

LOS ALAMOS NATIONAL LABORATORY
P.O. BOX 1663
LOS ALAMOS, NM 87545
  01CY ATTN DOC CON FOR J. WOLCOTT
  01CY ATTN DOC CON FOR R.F. TASCHEK
  01CY ATTN DOC CON FOR E. JONES
  01CY ATTN DOC CON FOR J. MALIK
  01CY ATTN DOC CON FOR R. JEFFRIES
  01CY ATTN DOC CON FOR J. ZINN
  01CY ATTN DOC CON FOR P. KEATON
  01CY ATTN DOC CON FOR D. WESTERVELT

SANDIA LABORATORIES
P.O. BOX 5800
ALBUQUERQUE, NM 87115
  01CY ATTN DOC CON FOR W. BROWN
  01CY ATTN DOC CON FOR A. THORNBROUGH
  01CY ATTN DOC CON FOR T. WRIGHT
  01CY ATTN DOC CON FOR D. DAHLGREN
  01CY ATTN DOC CON FOR 3141
  01CY ATTN DOC CON FOR SPACE PROJECT DIV

SANDIA LABORATORIES
LIVERMORE LABORATORY
P.O. BOX 969
LIVERMORE, CA 94550
  01CY ATTN DOC CON FOR B. MURPHEY
  01CY ATTN DOC CON FOR T. COOK

OFFICE OF MILITARY APPLICATION
DEPARTMENT OF ENERGY
WASHINGTON, D.C. 20545
  01CY ATTN DOC CON DR. YO SONG

OTHER GOVERNMENT

DEPARTMENT OF COMMERCE
NATIONAL BUREAU OF STANDARDS
WASHINGTON, D.C. 20234
  (ALL CORRES: ATTN SEC OFFICER FOR)
  01CY ATTN R. MOORE

INSTITUTE FOR TELECOM SCIENCES
NATIONAL TELECOMMUNICATIONS & INFO ADMIN
BOULDER, CO 80303
  01CY ATTN A. JEAN (UNCLASS ONLY)
  01CY ATTN W. UTLAUT
  01CY ATTN D. CROMBIE
  01CY ATTN L. BERRY

NATIONAL OCEANIC & ATMOSPHERIC ADMIN
ENVIRONMENTAL RESEARCH LABORATORIES
DEPARTMENT OF COMMERCE
BOULDER, CO 80302
  01CY ATTN R. GRUBB
  01CY ATTN AERONOMY LAB G. REID

DEPARTMENT OF DEFENSE CONTRACTORS

AEROSPACE CORPORATION
P.O. BOX 92957
LOS ANGELES, CA 90009
  01CY ATTN I. GARFUNKEL
  01CY ATTN T. SALMI
  01CY ATTN V. JOSEPHSON
  01CY ATTN S. BOWER
  01CY ATTN D. OLSEN

ANALYTICAL SYSTEMS ENGINEERING CORP
5 OLD CONCORD ROAD
BURLINGTON, MA 01803
  01CY ATTN RADIO SCIENCES

BERKELEY RESEARCH ASSOCIATES, INC.
P.O. BOX 983
BERKELEY, CA 94701
  01CY ATTN J. WORKMAN
  01CY ATTN C. PRETTIE
  01CY ATTN S. BRECHT

BOEING COMPANY, THE
P.O. BOX 3707
SEATTLE, WA 98124
  01CY ATTN G. KEISTER
  01CY ATTN D. MURRAY
  01CY ATTN G. HALL
  01CY ATTN J. KENNEY

CALIFORNIA AT SAN DIEGO, UNIV OF
P.O. BOX 6049
SAN DIEGO, CA 92106

CHARLES STARK DRAPER LABORATORY, INC.
555 TECHNOLOGY SQUARE
CAMBRIDGE, MA 02139
  01CY ATTN D.B. COX
  01CY ATTN J.P. GILMORE

COMSAT LABORATORIES
LINTHICUM ROAD
CLARKSBURG, MD 20734
  01CY ATTN G. HYDE

CORNELL UNIVERSITY
DEPARTMENT OF ELECTRICAL ENGINEERING
ITHACA, NY 14850
  01CY ATTN D.T. FARLEY, JR.

ELECTROSPACE SYSTEMS, INC.
BOX 1359
RICHARDSON, TX 75080
  01CY ATTN H. LOGSTON
  01CY ATTN SECURITY (PAUL PHILLIPS)

ESL, INC.
495 JAVA DRIVE
SUNNYVALE, CA 94086
  01CY ATTN J. ROBERTS
  01CY ATTN JAMES MARSHALL

GENERAL ELECTRIC COMPANY
SPACE DIVISION
VALLEY FORGE SPACE CENTER
GODDARD BLVD KING OF PRUSSIA
P.O. BOX 8555
PHILADELPHIA, PA 19101
  01CY ATTN M.H. BORTNER SPACE SCI LAB

GENERAL ELECTRIC COMPANY
P.O. BOX 1122
SYRACUSE, NY 13201
  01CY ATTN F. REIBERT

GENERAL ELECTRIC TECH SERVICES CO., INC.
HMES
COURT STREET
SYRACUSE, NY 13201
  01CY ATTN G. MILLMAN

GENERAL RESEARCH CORPORATION
SANTA BARBARA DIVISION
P.O. BOX 6770
SANTA BARBARA, CA 93111
  01CY ATTN JOHN ISE, JR.
  01CY ATTN JOEL GARBARINO

GEOPHYSICAL INSTITUTE
UNIVERSITY OF ALASKA
FAIRBANKS, AK 99701
  (ALL CLASS ATTN: SECURITY OFFICER)
  01CY ATTN T.N. DAVIS (UNCLASS ONLY)
  01CY ATTN TECHNICAL LIBRARY
  01CY ATTN NEAL BROWN (UNCLASS ONLY)

GTE SYLVANIA, INC.
ELECTRONICS SYSTEMS GRP-EASTERN DIV
77 A STREET
NEEDHAM, MA 02194
  01CY ATTN MARSHALL CROSS

HSS, INC.
2 ALFRED CIRCLE
BEDFORD, MA 01730
  01CY ATTN DONALD HANSEN

ILLINOIS, UNIVERSITY OF
107 COBLE HALL
150 DAVENPORT HOUSE
CHAMPAIGN, IL 61820
  (ALL CORRES ATTN DAN MCCLELLAND)
  01CY ATTN K. YEH

INSTITUTE FOR DEFENSE ANALYSES
400 ARMY-NAVY DRIVE
ARLINGTON, VA 22202
  01CY ATTN J.M. AEIN
  01CY ATTN ERNEST BAUER
  01CY ATTN HANS WOLFARD
  01CY ATTN JOEL BENGSTON

INTL TEL & TELEGRAPH CORPORATION
500 WASHINGTON AVENUE
NUTLEY, NJ 07110
  01CY ATTN TECHNICAL LIBRARY

JAYCOR
11011 TORREYANA ROAD
P.O. BOX 85154
SAN DIEGO, CA 92138
  01CY ATTN J.L. SPERLING

JOHNS HOPKINS UNIVERSITY
APPLIED PHYSICS LABORATORY
JOHNS HOPKINS ROAD
LAURAL, MD 20810
  01CY ATTN DOCUMENT LIBRARIAN
  01CY ATTN THOMAS POTEMRA
  01CY ATTN JOHN DASSOULAS

KAMAN SCIENCES CORP
P.O. BOX 7463
COLORADO SPRINGS, CO 80933
  01CY ATTN T. MEAGHER
KAMAN TEMPO-CENTER FOR ADVANCED STUDIES
816 STATE STREET (P.O DRAWER QQ)
SANTA BARBARA, CA 93102
  01CY ATTN DASIAC
  01CY ATTN TIM STEPHANS
  01CY ATTN WARREN S. KNAPP
  01CY ATTN WILLIAM MCNAMARA
  01CY ATTN B. GAMBILL

LINKABIT CORP
10453 ROSELLE
SAN DIEGO, CA 92121
  01CY ATTN IRWIN JACOBS

LOCKHEED MISSILES & SPACE CO., INC
P.O. BOX 504
SUNNYVALE, CA 94088
  01CY ATTN DEPT 60-12
  01CY ATTN D.R. CHURCHILL

LOCKHEED MISSILES & SPACE CO., INC.
3251 HANOVER STREET
PALO ALTO, CA 94304
  01CY ATTN MARTIN WALT DEPT 52-12
  01CY ATTN W.L. IMHOF DEPT 52-12
  01CY ATTN RICHARD G. JOHNSON DEPT 52-12
  01CY ATTN J.B. CLADIS DEPT 52-12

LOCKHEED MISSILE & SPACE CO., INC.
HUNTSVILLE RESEARCH & ENGR. CTR.
4800 BRADFORD DRIVE
HUNTSVILLE, AL 35807
  ATTN DALE H. DIVIS

MARTIN MARIETTA CORP
ORLANDO DIVISION
P.O. BOX 5837
ORLANDO, FL 32805
  01CY ATTN R. HEFFNER

M.I.T. LINCOLN LABORATORY
P.O. BOX 73
LEXINGTON, MA 02173
  01CY ATTN DAVID M. TOWLE
  01CY ATTN P. WALDRON
  01CY ATTN L. LOUGHLIN
  01CY ATTN D. CLARK

MCDONNEL DOUGLAS CORPORATION
5301 BOLSA AVENUE
HUNTINGTON BEACH, CA 92647
  01CY ATTN N. HARRIS
  01CY ATTN J. MOULE
  01CY ATTN GEORGE MROZ
  01CY ATTN W. OLSON
  01CY ATTN R.W. HALPRIN
  01CY ATTN TECHNICAL LIBRARY SERVICES

MISSION RESEARCH CORPORATION
735 STATE STREET
SANTA BARBARA, CA 93101
  01CY   ATTN P. FISCHER
  01CY   ATTN W.F. CREVIER
  01CY   ATTN STEVEN L. GUTSCHE
  01CY   ATTN D. SAPPENFIELD
  01CY   ATTN R. BOGUSCH
  01CY   ATTN R. HENDRICK
  01CY   ATTN RALPH KILB
  01CY   ATTN DAVE SOWLE
  01CY   ATTN F. FAJEN
  01CY   ATTN M. SCHEIBE
  01CY   ATTN CONRAD L. LONGMIRE
  01CY   ATTN WARREN A. SCHLUETER

MITRE CORPORATION, THE
P.O. BOX 208
BEDFORD, MA 01730
  01CY   ATTN JOHN MORGANSTERN
  01CY   ATTN G. HARDING
  01CY   ATTN C.E. CALLAHAN

MITRE CORP
WESTGATE RESEARCH PARK
1820 DOLLY MADISON BLVD
MCLEAN, VA 22101
  01CY   ATTN W. HALL
  01CY   ATTN W. FOSTER

PACIFIC-SIERRA RESEARCH CORP
12340 SANTA MONICA BLVD.
LOS ANGELES, CA 90025
  01CY   ATTN E.C. FIELD, JR.

PENNSYLVANIA STATE UNIVERSITY
IONOSPHERE RESEARCH LAB
318 ELECTRICAL ENGINEERING EAST
UNIVERSITY PARK, PA 16802
  (NO CLASS TO THIS ADDRESS)
  01CY   ATTN IONOSPHERIC RESEARCH LAB

PHOTOMETRICS, INC.
442 MARRETT ROAD
LEXINGTON, MA 02173
  01CY   ATTN IRVING L. KOFSKY

PHYSICAL DYNAMICS, INC.
P.O. BOX 3027
BELLEVUE, WA 98009
  01CY   ATTN E.J. FREMOUW

PHYSICAL DYNAMICS, INC.
P.O. BOX 10367
OAKLAND, CA 94610
  ATTN A. THOMSON

R & D ASSOCIATES
P.O. BOX 9695
MARINA DEL REY, CA 90291
  01CY   ATTN FORREST GILMORE
  01CY   ATTN WILLIAM B. WRIGHT, JR.
  01CY   ATTN ROBERT F. LELEVIER
  01CY   ATTN WILLIAM J. KARZAS
  01CY   ATTN H. ORY
  01CY   ATTN C. MACDONALD
  01CY   ATTN R. TURCO

RAND CORPORATION, THE
1700 MAIN STREET
SANTA MONICA, CA 90406
  01CY   ATTN CULLEN CRAIN
  01CY   ATTN ED BEDROZIAN

RAYTHEON CO.
528 BOSTON POST ROAD
SUDBURY, MA 01776
  01CY   ATTN BARBARA ADAMS

RIVERSIDE RESEARCH INSTITUTE
80 WEST END AVENUE
NEW YORK, NY 10023
  01CY   ATTN VINCE TRAPANI

SCIENCE APPLICATIONS, INC.
P.O. BOX 2351
LA JOLLA, CA 92038
  01CY   ATTN LEWIS M. LINSON
  01CY   ATTN DANIEL A. HAMLIN
  01CY   ATTN E. FRIEMAN
  01CY   ATTN E.A. STRAKER
  01CY   ATTN CURTIS A. SMITH
  01CY   ATTN JACK MCDOUGALL

SCIENCE APPLICATIONS, INC
1710 GOODRIDGE DR.
MCLEAN, VA 22102
  ATTN: J. COCKAYNE

SRI INTERNATIONAL
333 RAVENSWOOD AVENUE
MENLO PARK, CA 94025
  01CY ATTN DONALD NEILSON
  01CY ATTN ALAN BURNS
  01CY ATTN G. SMITH
  01CY ATTN L.L. COBB
  01CY ATTN DAVID A. JOHNSON
  01CY ATTN WALTER G. CHESNUT
  01CY ATTN CHARLES L. RINO
  01CY ATTN WALTER JAYE
  01CY ATTN M. BARON
  01CY ATTN RAY L. LEADABRAND
  01CY ATTN G. CARPENTER
  01CY ATTN G. PRICE
  01CY ATTN J. PETERSON
  01CY ATTN R. HAKE, JR.
  01CY ATTN V. GONZALES
  01CY ATTN D. MCDANIEL

STEWART RADIANCE LABORATORY
UTAH STATE UNIVERSITY
1 DE ANGELO DRIVE
BEDFORD, MA 01730
  01CY ATTN J. ULWICK

TECHNOLOGY INTERNATIONAL CORP
75 WIGGINS AVENUE
BEDFORD, MA 01730
  01CY ATTN W.P. BOQUIST

TRW DEFENSE & SPACE SYS GROUP
ONE SPACE PARK
REDONDO BEACH, CA 90278
  01CY ATTN R. K. PLEBUCH
  01CY ATTN S. ALTSCHULER
  01CY ATTN D. DEE
  01CY ATTN D/ Stockwell
              SNTF/1575

VISIDYNE
SOUTH BEDFORD STREET
BURLINGTON, MASS 01803
  01CY ATTN W. REIDY
  01CY ATTN J. CARPENTER
  01CY ATTN C. HUMPHREY

EOS TECHNOLOGIES, INC.
606 Wilshire Blvd.
Santa Monica, Calif 90401
  01CY ATTN C.B. GABBARD